Thermochimica Acta, 139 (1989) 169–179
Elsevier Science Publishers B.V., Amsterdam – Printed in The Netherlands

THERMODYNAMIC STUDIES OF THE HIGH TEMPERATURE SUPERCONDUCTOR $Ba_2TmCu_3O_7$ *

TOORU ATAKE, HITOSHI KAWAJI, SHOICHI TAKANABE and YASUTOSHI SAITO
Research Laboratory of Engineering Materials, Tokyo Institute of Technology, 4259 Nagatsuta-cho, Midori-ku, Yokohama 227 (Japan)

KAZUYA MORI and YUZO SAEKI
Kanagawa Institute of Technology, 1030 Shimo-Ogino, Atsugi, Kanagawa-ken 243-02 (Japan)
(Received 1 June 1988)

ABSTRACT

Heat capacity measurements have been made by adiabatic calorimetry between 7 and 300 K on the high temperature superconductor $Ba_2TmCu_3O_7$, which was prepared by the method of powder calcination and characterized by X-ray powder diffraction, electrical resistivity and magnetic susceptibility measurements. An anomaly due to the superconducting phase transition has been observed at 90.9 K, with a heat capacity jump of 5.1 J K^{-1} mol^{-1} from which the electronic heat capacity coefficient is calculated as 39 mJ K^{-2} mol^{-1} in the weak-coupling limit of the Bardeen–Cooper–Schrieffer theory. Electrical resistivities have also been measured precisely under the same conditions as used in the calorimetry, i.e. on the same sample maintained at thermodynamic equilibrium. In the transition region, curves of both the heat capacity anomaly and the resistivity drop have been compared in detail.

INTRODUCTION

Following the pioneering work by Bednorz and Müller [1] and the subsequent discovery of superconductivity above 90 K in $Ba_2YCu_3O_7$ [2–4], a series of compounds $Ba_2MCu_3O_7$ (where M is a rare earth element other than Ce, Pr, Tb) have also been found to exhibit superconductivity above 90 K. These compounds are known to be isostructural with the prototype compound $Ba_2YCu_3O_7$, i.e. they have an orthorhombic oxygen-deficient perovskite-like structure. Their properties seem not to be dependent on the kind of rare earth element [5], and are quite different from those of classical superconductors as shown by such physical properties as low critical current and insensitivity to the presence of paramagnetic ions, etc. [6–10]. Although some rare earth elements are strongly paramagnetic in the oxide ceramics,

* Dedicated to Professor Edgar F. Westrum, Jr., on the occasion of his 70th birthday and in honor of his contributions to calorimetry and thermal analysis.

0040-6031/89/$03.50

substitutions of such elements does not influence the superconductivity of these compounds. Such a situation poses an important question over whether the mechanism of the superconductivity can be elucidated on the basis of the BCS (Bardeen–Cooper–Schrieffer) theory. However, the question still remains open, and precise measurements of the thermodynamic properties are required for compounds synthesized as a high purity single phase.

Although the heat capacity measurements have been made extensively in the low temperature region [6–16] as well as in the transition region [17–21], accurate thermodynamic properties over the temperature range up to room temperature have not yet been established for well-synthesized samples. The present authors started a series of thermodynamic investigations of the high temperature superconductors in the fall of 1986, and have accumulated a store of precise data, some results of which have already been published [22–26]. In the present paper, the heat capacities are reported for well-synthesized $Ba_2TmCu_3O_7$. The electrical resistivities have also been measured under the same conditions as used in the calorimetry experiments. As the measurements have been made under precise thermodynamic equilibrium conditions, the data can be compared with the heat capacities in detail. The curve of the resistivity drop is superimposed on the graph of the heat capacity anomaly at the superconducting phase transition.

EXPERIMENTAL

Sample preparation

The sample of $Ba_2TmCu_3O_7$ was prepared by the method of powder calcination from a stoichiometric mixture of $Ba(NO_3)_2$, Tm_2O_3 and CuO. The high purity starting materials were purchased from Rare Metallic Co., Ltd.; the nominal purities were 99.99, 99.9 and 99.99% for $Ba(NO_3)_2$, Tm_2O_3 and CuO, respectively. The reactants were pulverized and mixed in an alumina mortar. The mixture was pressed into disks of 16 mm diameter and 5 mm thickness under 200 MPa. The disks were put into an electric furnace and heated up to 1173 K in an oxygen atmosphere. After firing for 4 h the disks were reground, pressed into disks and then heated again. This process was repeated. At the final stage, the sample was heated for 24 h and then cooled down stepwise. Later, the sample was annealed at 673 K for 4 h.

The products were identified as having the same structure as the prototype compound $Ba_2YCu_3O_7$ by X-ray powder diffraction with Ni-filtered Cu K_α radiation in which no impurities were detected. The surface of the disk was observed by a scanning electron microscope (model JSM-T300, JEOL Ltd.). Well-sintered particles of several μm diameter were clearly seen. The EPMA images also showed uniform distribution of Ba, Tm and Cu atoms. The oxygen deficiency of the sample was determined by iodomet-

ric titration, by which the exact formula was determined to be $Ba_2TmCu_3O_{6.96}$. In the present paper, however, the simplified expression $Ba_2TmCu_3O_7$ is used.

Heat capacity measurements

A laboratory-made adiabatic calorimeter was used for the heat capacity measurements from liquid helium temperature to 350 K. The calorimeter vessel was made of gold-plated copper and the total weight was 35 g including the lead wires, heater and thermometers. The working thermometers, mounted on the calorimeter vessel, consisted of a platinum resistance thermometer (type 5187L, H. Tinsley and Co., Ltd.) calibrated on the IPTS-68 between 13.81 and 373.15 K at the National Physical Laboratory, England, and a germanium resistance thermometer (model GR-200A-500, Lake Shore Cryotronics, Inc.) calibrated on the EPT-76 between 1.2 and 23 K. An a.c. automatic bridge (type 5840D, H. Tinsley and Co., Ltd.) with a precision of 0.0001 K was used for the platinum thermometer. The resistance of the germanium thermometer was measured with a high precision digital voltmeter (model TR-6871, Advantest Co.) and a universal scanner (model TR-7200). The measuring system was automated using a microcomputer (model PC-9801m2, NEC) through GP-IB. A more detailed description of the calorimeter will be published in a subsequent paper [27].

The disks of the sample were crushed into small particles a few mm in diameter and loaded into the calorimeter vessel. The vessel was evacuated and a small amount of helium gas (10 kPa at room temperature) was added to maintain thermal uniformity within the calorimeter vessel. The amount of the sample was 25.6312 g (0.034348 mol), which contributed about 60% of the total heat capacity. The contribution of the helium gas was negligible compared with the total heat capacity.

Electrical resistivity measurements

An apparatus was constructed for measuring precisely the electrical resistivity as well as a.c. magnetic susceptibilities between liquid helium temperature and 350 K. The cryostat was similar to that of the adiabatic calorimeter. The sample vessel was maintained at thermodynamic equilibrium using the automated adiabatic control system. The temperature was measured with a 27 Ω rhodium–iron resistance thermometer (Cryogenic Calibration Ltd.) calibrated on the IPTS-68 between 1.5 and 293 K.

The disk of the sample was cut and shaped into a $3 \times 4 \times 15$ mm tetragonal prism, and copper wires 0.1 mm in diameter were attached with silver paste (no. 13, Engelhard Industries K. K.) for the four-terminal method. A digital voltmeter (Advantest Co., model TR-6871) and a univer-

TABLE 1. Measured molar heat capacities of $Ba_2TmCu_3O_7$

T (K)	C_p (J K^{-1} mol^{-1})	T (K)	C_p (J K^{-1} mol^{-1})	T (K)	C_p (J K^{-1} mol^{-1})
Series 1		145.29	201.03	10.72	0.86
60.20	84.45	147.32	202.92		
61.93	87.85	149.38	205.02	Series 3	
63.64	91.12	151.43	206.81	8.09	0.46
65.38	94.54	143.48	208.66	8.78	0.54
67.13	97.78	155.53	210.51	9.43	0.63
68.87	101.22	157.59	212.34	10.07	0.73
70.60	104.27	159.66	214.46	10.76	0.87
72.35	107.59	161.73	216.04	11.45	1.01
74.08	110.64	163.79	217.82	12.18	1.18
75.83	113.94	165.85	219.60	12.88	1.36
77.59	117.14	167.91	221.48	13.56	1.61
79.34	120.22	169.96	222.92		
81.09	123.31	172.03	224.61	Series 4	
82.84	126.51	174.18	226.33	8.38	0.50
84.59	129.58	176.39	228.12	9.14	0.59
86.34	133.06	178.59	229.95	9.87	0.70
88.09	136.11	180.78	231.35	10.53	0.82
89.88	138.75	182.96	232.98	11.21	0.96
91.67	139.01	185.12	234.59	11.99	1.13
93.48	140.23	187.28	236.25	12.80	1.36
95.28	142.63	189.42	237.52	13.62	1.64
97.07	144.82	191.55	238.98	14.49	2.00
98.86	147.31	193.67	240.35	15.47	2.45
100.64	149.56	195.78	241.97	16.55	3.14
102.42	152.00	197.88	243.25	12.80	1.36
104.21	154.44	199.97	244.50	13.62	1.64
106.01	156.63	202.05	245.91	14.49	2.00
107.80	158.93	204.12	247.19		
109.61	161.22	206.18	248.68	Series 5	
111.44	163.51	208.23	249.71	14.18	1.81
113.27	165.87	210.28	250.97	15.21	2.30
115.10	167.91	212.32	252.22	16.32	2.91
116.93	170.18	214.34	253.34	17.47	3.68
118.77	172.33	216.36	254.59	18.69	4.71
120.60	174.51	218.38	255.66	19.97	5.97
122.44	176.73	220.41	256.77	21.24	7.36
124.31	178.86	222.50	257.98	22.53	8.96
126.19	180.95	224.60	259.27	23.90	10.82
128.07	182.98	226.70	260.18	25.33	12.92
129.95	185.11	228.79	261.20	26.74	15.28
131.84	187.38	230.90	262.27	28.12	17.67
133.73	189.13	233.04	263.47	29.50	20.17
135.62	191.11	235.17	264.44	30.97	22.98
137.51	193.11	237.29	265.34	32.53	26.02
139.40	195.08			34.15	29.32
141.33	197.21	Series 2		35.78	32.74
143.30	199.09	8.56	0.52	37.44	36.28

TABLE 1 (continued)

T (K)	C_p ($J\,K^{-1}\,mol^{-1}$)	T (K)	C_p ($J\,K^{-1}\,mol^{-1}$)	T (K)	C_p ($J\,K^{-1}\,mol^{-1}$)
39.06	39.71	102.79	152.30	99.63	148.19
40.69	43.24	103.70	153.47	100.16	148.79
42.40	47.02	104.60	154.67	100.69	149.54
44.13	50.67	105.49	156.02	101.22	150.25
45.87	54.52	106.38	157.26	101.74	150.92
47.54	58.09	107.26	158.19	102.26	151.77
49.20	61.65			102.78	152.40
50.93	65.36	Series 6		103.30	152.88
52.71	69.05	72.58	107.91	103.82	153.80
54.49	72.77	75.02	112.41	104.33	154.28
56.29	76.51	76.42	114.93	104.84	154.87
58.13	80.23	77.10	116.15	105.35	155.95
59.96	83.92	77.78	117.35	105.86	156.35
61.76	87.48	78.45	118.62	106.37	156.88
63.52	90.93	79.12	119.64	106.87	157.56
65.28	94.37	79.78	121.05	107.37	158.50
66.87	97.30	80.43	122.20	108.00	159.24
68.28	99.94	81.08	123.09	108.81	160.30
69.65	102.59	81.72	124.46	109.67	161.24
70.98	104.95	82.35	125.66		
72.29	107.39	82.99	126.50	Series 7	
73.56	109.79	83.61	127.89	235.88	264.66
74.82	111.98	84.23	128.82	238.25	265.83
76.04	114.27	84.85	129.99	240.60	266.90
77.25	116.51	85.46	131.25	242.95	268.15
78.43	118.50	86.06	132.29	245.30	269.03
79.60	120.69	86.66	133.28	247.63	269.97
80.74	122.71	87.26	134.61	249.95	270.93
81.86	124.55	87.85	135.80	252.27	272.25
82.97	126.69	88.44	136.61	254.60	272.93
84.07	128.60	89.03	137.63	256.95	273.86
85.15	130.65	89.61	138.51	259.28	274.87
86.21	132.66	90.18	139.07	261.62	275.91
87.26	134.54	90.76	139.21	263.94	276.73
88.29	136.53	91.33	139.06	266.26	277.75
89.32	138.10	91.91	138.63	268.57	278.57
90.33	138.97	92.47	139.20	270.87	279.54
91.34	139.02	93.04	139.60	273.17	280.19
92.33	138.96	93.61	140.10	275.46	281.46
93.33	139.90	94.17	141.17	277.75	282.34
94.31	141.21	94.73	141.55	280.03	282.83
95.28	142.43	95.28	142.50	282.30	283.79
96.25	143.61	95.83	143.01	284.57	284.13
97.21	145.00	96.38	143.90	286.83	284.86
98.16	146.15	96.93	144.62	289.09	285.68
99.10	147.37	97.48	145.19	291.34	286.61
100.03	148.69	98.02	146.03	293.58	287.35
100.96	149.88	98.56	146.55	298.04	288.50
101.88	151.23	99.09	147.31	300.31	289.52

sal scanner (TR-7200) equipped with GP-IB were used for the automatic measurements by using a microcomputer (PC9801Vm2, NEC).

RESULTS AND DISCUSSION

Heat capacities

The heat capacities were measured for the ceramic sample of $Ba_2TmCu_3O_7$ between 7 and 300 K. During the experiments, no abnormal relaxation or hysteresis phenomena were observed. It took a few minutes to achieve a temperature step of about 1 K for measurements in the lowest temperature region. However, this energy-input time was increased as the temperature increased, becoming 10 minutes for an increment of about 1.5 K above 100 K. After the heat input was complete, thermal equilibrium within the calorimeter vessel was attained in a few minutes below 20 K, 5 min at about 50 K and 10 min above 100 K. Thus, the time needed for a heat capacity measurement varied with temperature depending on the heat capacities and thermal conductivities; a few minutes below 20 K to half an hour near room temperature.

The measured molar heat capacities without curvature corrections are shown in Fig. 1, and tabulated in Table 1. As the data are listed in a chronological order, the temperature increment due to each energy input is estimated from the adjacent mean temperatures which are close enough to neglect the curvature corrections compared with the experimental precision. The smoothed values of molar heat capacities obtained from the present results are given in Table 2.

In Fig. 1, a typical second-order type of anomaly can be seen clearly at about 90 K, which coincides with the electrical resistivity drop caused by the

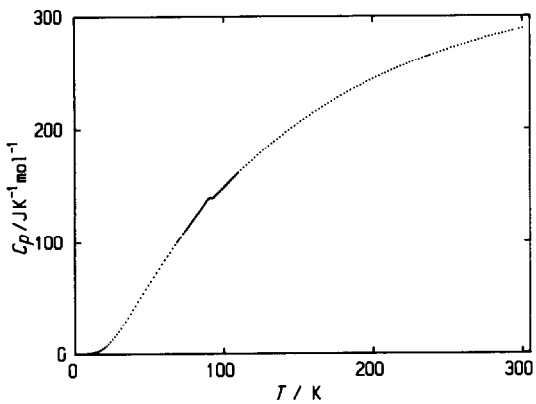

Fig. 1. Measured molar heat capacities of $Ba_2TmCu_3O_7$.

TABLE 2

Smoothed values of molar heat capacities of $Ba_2TmCu_3O_7$ at rounded temperatures

T (K)	C_p (J K^{-1} mol^{-1})	T (K)	C_p (J K^{-1} mol^{-1})
8	0.46	110	161.67
10	0.72	120	173.84
15	2.19	130	185.17
20	5.98	140	195.71
25	12.47	150	205.49
30	21.11	160	214.56
35	31.10	170	222.99
40	41.76	180	230.81
45	52.63	190	238.01
50	63.35	200	244.67
55	73.83	210	250.83
60	84.00	220	256.56
65	93.78	230	261.83
70	103.19	240	266.63
75	112.35	250	271.05
80	121.39	260	275.21
85	130.35	270	279.15
90	138.89	280	282.77
95	142.04	290	287.07
100	148.57	300	289.11
105	155.24		

superconducting phase transition. The heat capacity curve seems to approach the classical limiting value of $39R \approx 324$ J K^{-1} mol^{-1} asymptotically above room temperature.

Superconducting phase transition

A magnified graph is given for the heat capacity anomaly due to the superconducting phase transition in Fig. 2, where the data of two independent series of measurements are plotted. The temperature step between each measurement is about 0.5 K. The critical temperature T_c of the superconducting phase transition is determined to be 90.9 K, at which the heat

TABLE 3

Properties of the superconducting phase transitions of $Ba_2MCu_3O_7$ (M = Dy, Er, Tm)

M	T_c (K)	γ (mJ K^{-2} mol^{-1})
Dy	92.5	29
Er	91.2	35
Tm	90.9	39

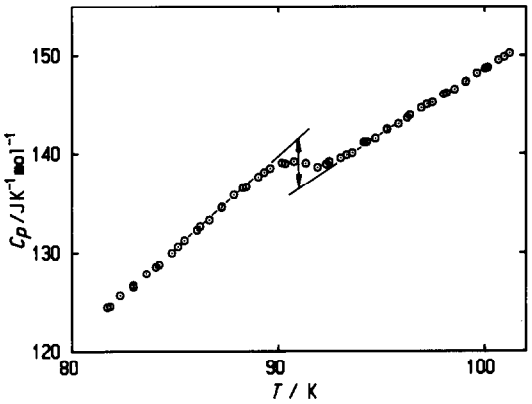

Fig. 2. Heat capacity anomaly due to the superconducting phase transition of $Ba_2TmCu_3O_7$.

capacity jump ΔC_p is 5.1 J K^{-1} mol^{-1} as shown by arrows in Fig. 2. According to the BCS theory, the electronic heat capacity coefficient γ is estimated at 39 mJ K^{-2} mol^{-1} in the weak-coupling limit; $\Delta C_p = 1.43\gamma T_c$. The value of γ is favorably comparable with the previous results [24–26,28,29] as given in Table 3. Although the sample with M = Dy has the highest T_c, its γ value is the smallest of other M. However, the shape of the anomaly for M = Dy is very clear and sharp compared with those of the others [24,26,28,29]. To clarify the reason for such a discord, further systematic investigations are required for the series of compounds substituted with other lanthanoids. Work along this line is in progress in our laboratory.

Electrical resistivities

The electrical resistivities were measured for the same sample of $Ba_2TmCu_3O_7$ under the same conditions as the calorimetry between 60 and

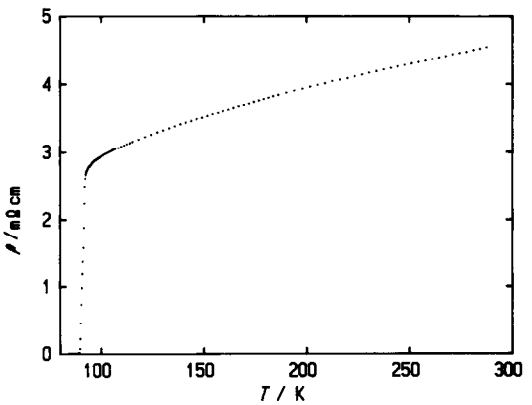

Fig. 3. Electrical resistivities of $Ba_2TmCu_3O_7$.

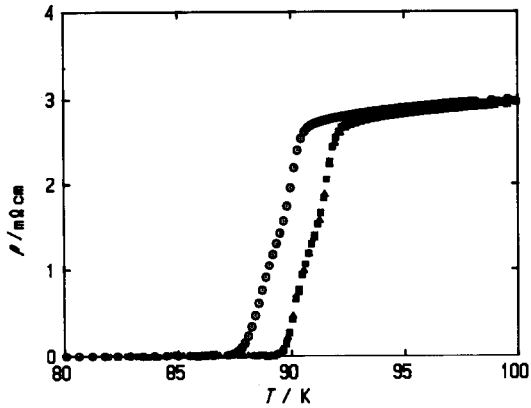

Fig. 4. Current dependences of the electrical resistivities of $Ba_2TmCu_3O_7$. ⊙, 30 mA; ▲, 4 mA; ■, 0.4 mA.

300 K. Figure 3 shows the data of a typical series of measurements. As the shape of the tetragonal prism of the sample and the location of the electrode wires on the surface of the sample were not fixed, the absolute value of the resistivity (the vertical scale in Fig. 3) is somewhat arbitrary. The data obtained with three different electrical currents are shown in Fig. 4 on an enlarged scale. The data at 30 mA are shifted to lower temperature compared with the others at 4 and 0.4 mA. The reason for these discrepancies must be the contact resistance of the electrodes (ca. 10 Ω). The data obtained with currents less than 4 mA coincide with each other within experimental precision, that is considered as intrinsic properties of the sample.

Thus, it is very interesting to compare the heat capacity anomaly with the electrical resistivity drop at the superconducting phase transition. The re-

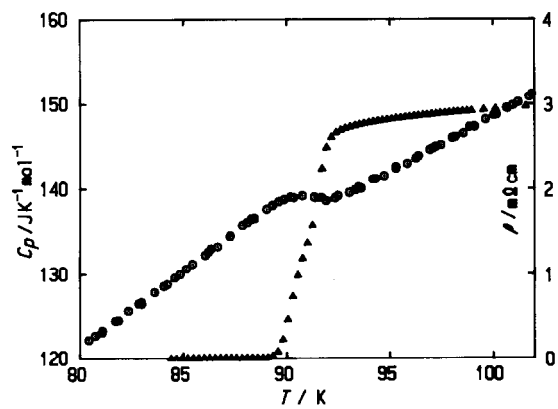

Fig. 5. Heat capacity anomaly and resistivity drop at the superconducting phase transition of $Ba_2TmCu_3O_7$.

sults of such a comparison are given in Fig. 5. The higher temperature end of the anomaly corresponds to the starting point of the resistivity drop. The midpoint of resistivity drop is at 90.9 K, which is the T_c obtained by calorimetry. A more detailed analysis and comparison of the two data should bring forth further information about the mechanism of the superconducting phase transition, and will be published shortly.

ACKNOWLEDGMENT

The authors would like to thank Dr. Yoshiki Takagi for the determination of oxygen deficiency of the sample by iodometric titration.

REFERENCES

1 J.G. Bednorz and K.K. Müller, Z. Phys. B, 64 (1986) 189.
2 M.K. Wu, J.R. Ashburn, C.J. Torng, P.H. Hor, R.L. Meng, L. Gao, Z.J. Huang, Y.Q. Wang and C.W. Chu, Phys. Rev. Lett., 59 (1987) 908.
3 Z.X. Zhao, L.Q. Chen, Q.S. Yang, Y.Z. Huang, G.H. Chen, R.M. Tang, G.R. Liu, C.G. Cui, L. Chen, L.Z. Wang, S.Q. Guo, L.S. Li and J.Q. Bi, Kexue Tongbao, 33 (1987) 661.
4 S. Hikami, T. Hirai and S. Kagoshima, Jpn. J. Appl. Phys., 26 (1987) L314.
5 T.J. Kistenmacher, Solid State Commun., 65 (1988) 981.
6 B.D. Dunlap, M. Slaski, D.G. Hinks, L. Soderholm, M. Beno, K. Zhang, C. Segre, G.W. Crabtree, W.K. Kwok, S.K. Malik, Ivan K. Schuller, J.D. Jorgensen and Z. Sungaila, J. Magn. Magn. Mater., 68 (1987) L139.
7 S. Simizu, S.A. Friedberg, E.A. Hayri and M. Greenblatt, Phys. Rev. B, 36 (1987) 7129.
8 A.P. Ramirez, L.F. Schneemeyer and J.V. Waszczak, Phys. Rev. B, 36 (1987) 7145.
9 J.M. Ferreira, B.W. Lee, Y. Dalichaouch, M.S. Torikachvili, K.N. Yang and M.B. Maple, Phys. Rev. B, 37 (1987) 1580.
10 B.W. Lee, J.M. Ferreira, Y. Dalichaouch, M.S. Torikachvili, K.N. Yang and M.B. Maple, Phys. Rev. B, 37 (1988) 2368.
11 J. van den Berg, C.J. van der Beek, P.H. Kes, J.A. Mydosh, G.J. Nieuwenhuys and L.J. de Jong, Solid State Commun., 64 (1987) 699.
12 S.J. Collocott, G.K. White, S.X. Dou and R.K. Williams, Phys. Rev. B, 36 (1987) 5684.
13 M.W. Reeves, D.S. Citrin, B.G. Pazol, T.A. Friedmann and D.M. Ginsberg, Phys. Rev. B, 36 (1987) 6915.
14 M.W. Dirken and L.J. de Jongh, Solid State Commun., 64 (1987) 1201.
15 B.D. Dunlap, M. Slaski, Z. Sungaila, D.G. Hinks, K. Zhang, C. Segre, S.K. Malik and E.E. Alp, Phys. Rev. B, 37 (1988) 592.
16 K. Kumagai, Y. Nakamichi, I. Watanabe, Y. Nakamura, H. Nakajima, N. Wada and P. Lederer, Phys. Rev. Lett., 60 (1988) 724.
17 Z. Chen, Y. Zhao, H. Yang, Z. Chen, D. Zheng, Y. Qian, B. Wu and Q. Zhang, Solid State Commun., 64 (1987) 685.
18 S.E. Inderhees, M.B. Salamon, T.A. Friedmann and D.M. Ginsberg, Phys. Rev. B, 36 (1987) 2401.
19 A. Junod, A. Bezinge and J. Muller, Physica C, 152 (1988) 50.
20 R.A. Butera, Phys. Rev. B, 37 (1988) 5909.

21 S.E. Inderhees, M.B. Salamon, N. Goldenfeld, J.P. Rice, B.G. Pazol, D.M. Ginsberg, J.Z. Liu and G.W. Crabtree, Phys. Rev. Lett., 60 (1988) 1178.
22 K. Kitazawa, T. Atake, M. Sakai, S. Uchida, H. Takagi, K. Kishio, T. Hasegawa, K. Fueki, Y. Saito and S. Tanaka, Jpn. J. Appl. Phys., 26 (1987) L751.
23 K. Kitazawa, T. Atake, H. Ishii, H. Sato, T. Takagi, S. Uchida, Y. Saito, K. Fueki and S. Tanaka, Jpn. J. Appl. Phys., 26 (1987) L748.
24 Y. Saito, T. Nakamura and T. Atake, Mat. Res. Soc. Symp. Proc., 99 (1988) 475.
25 T. Atake, Y. Takagi, T. Nakamura and Y. Saito, Phys. Rev., B37 (1988) 552.
26 Y. Saito and T. Atake, Rep. RLEMTIT., 13 (1988) 12.
27 T. Atake, H. Kawaji, A. Hamano and Y. Saito, in preparation.
28 T. Atake, Y. Takagi, H. Kawaji, T. Nakamura and Y. Saito, in preparation.
29 T. Atake, K. Kitazawa, K. Kishio, H. Takagi and Y. Saito, in preparation.